

An Analytical Method for Calculating Radiated Emission of Discontinuous Penetrating Cable

Bing-Xue Zhang¹, Pei Xiao¹, Dan Ren², and Ping-An Du¹

¹ School of Mechanical and Electrical Engineering
University of Electronic Science and Technology of China, Chengdu 611731, China
bingxuezhang@163.com, xiaopei_uestc@sina.cn, dupingan@uestc.edu.cn

² Institute of Electronic Engineering
China Academy of Engineering Physics, Mianyang 621900, China
rendan_uestc@163.com

Abstract — Since the interconnection cable between devices is usually much longer than those inside an enclosure, it provides a main gateway for radiated interference. An analytical method for calculating the radiated field of penetrating cable including connectors is proposed based on the cascaded network. This method takes into account the effect of connectors on signal transmission in the calculation model. The discontinuous penetrating cable is regarded as two-port cascaded model which includes three parts: internal cables inside enclosure, connectors and an external cable. The terminal voltage and current of the cable are determined according to terminal conditions, and the current distribution is solved by the transmission line theory. Finally, the electromagnetic radiation of discontinuous penetrating cable is obtained by dipole approximation method. The proposed method is verified by numerical simulation.

Index Terms — Cable-enclosure system, cascaded network, connector, discontinuous penetrating cable, radiated emission.

I. INTRODUCTION

A cable is widely used as a connection between separate electronic devices for data or energy transmission. Due to the antenna effect, cable probably radiates considerable emission during signal transmission through it, and therefore produces significant electromagnetic interference. Thus, how to predict and control the radiated emission from cable has gained much attention, and so far, some calculation approaches have been put forward.

Meyer *et al.* proposed a calculation method of the radiated field for the interconnection cable between a power converter and a motor, which utilized the transmission line theory to obtain the current distribution along a cable, then used the electric field integral equation and the mirror theory to solve the radiated field where complex 3D modeling was avoided [1]. Xu *et al.*

used several Hertzian dipoles as the equivalency of a multi-conductor transmission line and combined the current distribution of each dipole to analyze the radiated emission of cable bundle [2]. Jia *et al.* used a RF current probe to measure the amplitude of the common-mode current and obtained the phase of the current based on the phase extraction method [3], which replaced the anechoic chamber to predict the radiated emission of a cable bundle. They also used the current time-domain scanning and fast Fourier transform to determine the amplitude and phase of current to improve the accuracy of phase extraction and the quality of radiation prediction [4].

For electromagnetic radiation of a cable-enclosure system, Wang proposed a method based on asymmetrical dipole approximation and common-mode current simulation to estimate the radiation of cable connected to conductive shell [5]. However, this method can only be used for radiation estimation of simple structures, and there are still some limitations in the application. Park *et al.* presented an alternative method by measuring the common-mode current on cable to determine the equivalent source between cable and box, and computed the radiation transfer function to predict the radiated emission of box-source-cable [6]. Costa *et al.* employed an equivalent circuit model to compute the current distribution of a cable bundle and further estimate the near-field radiation [7]. However, it is rather difficult to create the exact circuit model of the device under test (EUT). Meng *et al.* considered the influence of connectors and supporting plates at both ends of the cable. Based on the dipole approximation method and the frequency domain analysis method of the transmission line, a fast calculation method was proposed for calculating the radiated emission of wire [8,9]. Jia *et al.* adopted the current scanning method and considered the radiation contribution of load structure to predict the radiation of the automotive system [10].

In practical problems, cable usually cannot be used to connect the excitation and load inside enclosures directly, but via the connectors mounted on the wall of enclosures, as shown in Fig. 1. The electrical connection function of the transmission system is realized through the mechanical engagement of pins and jacks in connector, where the contact resistance, inductance, conductance and capacitance exist and the consequent waveform distortion or even errors may occur. Thus, a cable may be divided by connectors into two parts, the external part (interconnection cable) and the internal parts (inside enclosure), so called discontinuous penetrating cable.

However, most of the present methods usually take the cable alone into account, and connectors are not included in calculation models. Since the connector impedance has considerable effect on signal transmission, which in turn affects the overall radiation of a cable-enclosure system, and thus, this paper presents a method for calculating radiated emissions of a discontinuous penetrating cable with connectors.

In the following part of the paper, Section II establishes the model of the discontinuous penetrating cable to solve the current distribution. In Section III, the radiation field approximation method is introduced and the radiated field of a cable-enclosure system is obtained. Section IV compares the method with the full-wave software CST to confirm the validation of the proposed method. And finally, some conclusions are drawn in Section V.

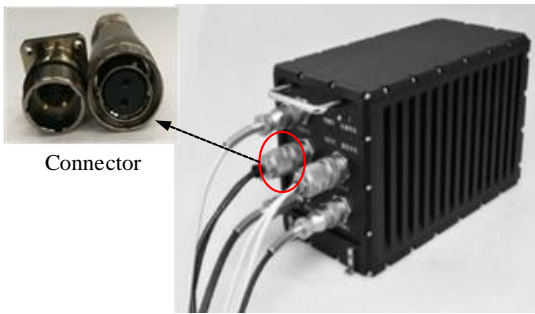


Fig. 1. A cable-enclosure system.

II. ESTABLISHMENT OF DISCONTINUOUS PENETRATING CABLE MODEL

A. Transmission parameter model of discontinuous penetrating cable

The model of a cable-enclosure system is shown in Fig. 2, which consists of an EUT and a load case with a printed circuit board (PCB), an interconnection cable connected with two internal cables through connectors between two enclosures. Within the system, radiation may be caused by the interconnection cable, internal

cables and PCB. High frequency signal on the PCB may be coupled to the cable, the radiation from the cable is dominant, and thus, the radiation of PCB is often neglected.

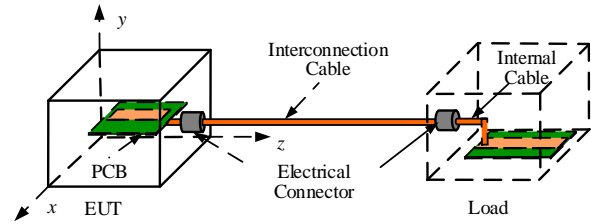


Fig. 2. The model of a cable-enclosure system.

During analysis, the radiation of cable is derived from the trace on the board. The electromagnetic radiation of PCB is mainly caused by common-mode current, while the radiation caused by differential-mode current can be neglected. Thus, a PCB with an attached cable can be modeled as an equivalent common-mode voltage source at junction between the cable and plate [11,12], as illustrated in Fig. 3. The voltage-driven principle is to couple electric field to connecting cable to generate a common-mode current. Shim [11] also presented the expression for the common-mode voltage with:

$$V_{cm} = \frac{C_{trace}}{C_{board}} V_{DM}, \quad (1)$$

where C_{trace} , C_{board} are the capacitance of trace and board, respectively, V_{DM} the signal voltage source.

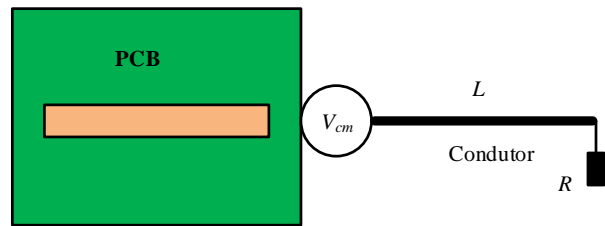


Fig. 3. Equivalent model of voltage-driven.

In the load case, the PCB terminal is connected to an impedance-matched load Z_L . Xiao [14] used a frequency-dependent lumped load Z_{eq} to replace the PCB, the equivalent load can be written as:

$$Z_{eq} = R' + Z_L. \quad (2)$$

Where R' is the resistance of trace, $R' = L_{rc}/wt\sigma$ [13].

Since the load impedance Z_L is matched with the characteristic impedance Z_m of the trace, they satisfy $Z_L = Z_m$, so Z_m can be expressed by:

$$Z_m = \begin{cases} \frac{60}{\sqrt{\epsilon_{re}}} \frac{1}{2\pi} \ln\left(\frac{8h+w}{w} + \frac{w}{4h}\right) & \frac{w}{h} \leq 1 \\ \frac{120\pi}{\sqrt{\epsilon_{re}}} \left[\frac{w}{h} + 1.393 + 0.667 \ln\left(\frac{w}{h} + 1.444\right) \right]^{-1} & \frac{w}{h} \geq 1 \end{cases}. \quad (3)$$

Where ϵ_{re} is the effective relative permittivity, w and h are the width and height of the trace, respectively.

Now, a discontinuous penetrating cable model, shown in Fig. 4, can be extracted from the cable-enclosure system, which includes EUT's internal cable l_0 , electrical connector a and b, interconnection cable l_2 , load enclosure internal cable l_4 , equivalent voltage V_{cm} , and equivalent load Z_{eq} .

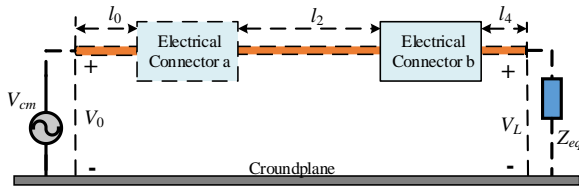


Fig. 4. A discontinuous penetrating cable model.

B. Calculation of current distribution

In general, if we are more interested in the output voltage and current of a complex circuit rather than its internal structure, the circuit can be regarded as a two-port network [13]. Thus, each part of the discontinuous penetrating cable model can be equivalent to a two-port circuit model, and a transmission matrix can be used to describe the relationship between the input and output voltage and current of each port. The expression can be expressed by:

$$\begin{pmatrix} V_i \\ I_i \end{pmatrix} = \begin{pmatrix} A_i & B_i \\ C_i & D_i \end{pmatrix} \begin{pmatrix} V_{i+1} \\ I_{i+1} \end{pmatrix}. \quad (4)$$

Where V_i and I_i ($i=0, 1, 2, 3, 4$) represent the voltage and current at the ports of internal cable of an EUT, connector a, interconnection cable, connector b and internal cable of load enclosure, respectively. A_i, B_i, C_i, D_i are transmission matrix parameters.

Assuming all cables are of the same type, the electrical parameters of interconnection and internal cable are consistent. Therefore, the transmission matrix of cables can be written as:

$$\begin{pmatrix} A_i & B_i \\ C_i & D_i \end{pmatrix} = \begin{pmatrix} \cosh(\gamma l_i) & Z_c \sinh(\gamma l_i) \\ \sinh(\gamma l_i)/Z_c & \cosh(\gamma l_i) \end{pmatrix} \quad i=0,2,4. \quad (5)$$

Where l_i is the length of each part of the cable.

To facilitate the study of a two-port cascaded network, we need to determine connector's scattering parameter first, which can be measured by a vector network analyzer (VNA) or computed by a numerical method. Then the transmission parameter matrix of connectors can be calculated by:

$$\begin{pmatrix} A_i & B_i \\ C_i & D_i \end{pmatrix} = \begin{pmatrix} \frac{(1+S_{11})(1-S_{22})+S_{12}S_{21}}{2S_{21}} & \frac{Z_{02}[(1+S_{11})(1+S_{22})-S_{12}S_{21}]}{2S_{21}} \\ \frac{[(1-S_{11})(1-S_{22})-S_{12}S_{21}]}{2S_{21}Z_{01}} & \frac{[(1-S_{11})(1+S_{22})+S_{12}S_{21}]Z_{01}}{2S_{21}Z_{02}} \end{pmatrix} \quad i=1,3. \quad (6)$$

Where Z_{01} and Z_{02} are the reference impedance of a connector port 1 and port 2, respectively.

By assembling each two-port network together, a cascade network of discontinuous penetrating cable can be formed as shown in Fig. 5, and by multiplying a series of matrix, the transmission matrix of the whole discontinuous penetrating cable system can be written as:

$$\begin{pmatrix} A & B \\ C & D \end{pmatrix} = \begin{pmatrix} A_0 & B_0 \\ C_0 & D_0 \end{pmatrix} \begin{pmatrix} A_1 & B_1 \\ C_1 & D_1 \end{pmatrix} \begin{pmatrix} A_2 & B_2 \\ C_2 & D_2 \end{pmatrix} \begin{pmatrix} A_3 & B_3 \\ C_3 & D_3 \end{pmatrix} \begin{pmatrix} A_4 & B_4 \\ C_4 & D_4 \end{pmatrix}. \quad (7)$$

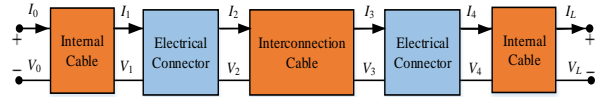


Fig. 5. A cascaded two-port network.

So, the relationship between an input and an output voltages and currents of the near and the far terminals is as follows:

$$\begin{pmatrix} V_0 \\ I_0 \end{pmatrix} = \begin{pmatrix} A & B \\ C & D \end{pmatrix} \begin{pmatrix} V_L \\ I_L \end{pmatrix}. \quad (8)$$

For a two-port network driven by the Thevenin circuit, the transmission parameters can be used to represent the load terminal voltage V_L and current I_L that can be calculated by:

$$\begin{cases} I_L = \frac{V_{cm}}{AZ_L + B} \\ V_L = \frac{Z_L V_{cm}}{AZ_L + B} \end{cases}. \quad (9)$$

The interconnection cable is the major source of radiated emission due to its relatively long length. The voltage and current of the interconnection cable l_2 are obtained by:

$$\begin{cases} V_4 = A_4 V_L + B_4 I_L = (A_4 Z_L + B_4) I_L \\ I_4 = C_4 V_L + D_4 I_L = (C_4 Z_L + D_4) I_L \end{cases}, \quad (10)$$

$$\begin{cases} V_3 = A_3 V_4 + B_3 I_4 \\ I_3 = C_3 V_4 + D_3 I_4 \end{cases}, \quad (11)$$

$$\begin{cases} V_2 = A_2 V_3 + B_2 I_3 \\ I_2 = C_2 V_3 + D_2 I_3 \end{cases}. \quad (12)$$

According to the transmission line theory, if the voltage V_2 and current I_2 at the initial end of the interconnection cable are available, the current distribution at any point can be expressed as:

$$I_2(z) = \frac{1}{2Z_c}(V_2 + I_2 Z_c)e^{-\gamma z} - \frac{1}{2Z_c}(V_2 - I_2 Z_c)e^{\gamma z}, \quad (13)$$

III. THE ANALYTICAL METHOD FOR RADIATED EMISSION OF DISCONTINUOUS PENETRATING CABLE

A. Dipole approximation method for cable radiated field

As a highly efficient transmitting antenna, a cable can propagate interference into surrounding space in the form of electromagnetic waves when the frequency of signal transmission exceeds 30MHz. Since antenna radiation is a macroscopic electromagnetic field problem, the rigorous analytical method can be used to solve Maxwell equations with different boundary conditions, but it may lead to mathematical complexity and lower efficiency. Therefore the Hertzian dipole approximation method is often used to predict cable radiated emission.

The following set of equations defines the radiated field generated by a dipole $I(z)dz$ at point A on a cable in Cartesian coordinate [16]:

$$\begin{cases} dE_x = e_x \left\{ -j \frac{I(z)dz}{4\pi\omega\epsilon} \frac{e^{-jkr}}{r^2} \sin\theta \cos\theta \cos\phi [3jk - rk^2 + \frac{3}{r}] \right\} \\ dE_y = e_y \left\{ -j \frac{I(z)dz}{4\pi\omega\epsilon} \frac{e^{-jkr}}{r^2} \sin\theta \cos\theta \sin\phi [3jk - rk^2 + \frac{3}{r}] \right\} \\ dE_z = e_z \left\{ j \frac{I(z)dz}{4\pi\omega\epsilon} \frac{e^{-jkr}}{r^2} [(jk - rk^2 + \frac{1}{r})\sin^2\theta - (2jk + \frac{2}{r})\cos^2\theta] \right\} \end{cases}, \quad (14)$$

where $k = \omega\sqrt{\mu\epsilon}$ is phase constant, ω angular frequency, r the distance from dipole to observation point P ; $\epsilon_0 = 8.85 \times 10^{-12}$ A/m and $\mu = 4\pi \times 10^{-7}$ A/m the permittivity and permeability for free space, respectively, θ the angle between AP connection and z axis, ϕ the angle between AP plane and z axis.

The electric field generated by the interconnection cable at the observation point P is E_{TL} , which is formed by the superposition of the electric fields by all the Hertzian dipoles on the cable, is:

$$E_{TL} = e_x \int_0^l dE_x + e_y \int_0^l dE_y + e_z \int_0^l dE_z. \quad (15)$$

Similarly, the electric field E'_{TL} formed by the mirror line of interconnection cable can also be calculated. Thus, the total electric field generated by interconnection cable is expressed as:

$$E = E_{TL} + E'_{TL}. \quad (16)$$

B. Analysis of the radiated field of cable-enclosure system

Because the surface current of enclosure is complex to calculate, its radiation contribution is difficult to obtain accurately. If the EUT and load enclosure are small compared to wavelength at frequency of interests and placed directly on the ground, the enclosure can be

modeled as a vertical monopole antenna model [8], as shown in Fig. 6, so we have:

$$\begin{cases} I_{d1} = I'_{d1} = I_2 \cdot n_y \\ I_{d2} = I'_{d2} = I_3 \cdot n_y \end{cases}. \quad (17)$$

Where I_{d1} and I'_{d1} are the real and mirror current of EUT side enclosure panel, respectively, I_{d2} and I'_{d2} are the real and mirror current of the load side enclosure panel.

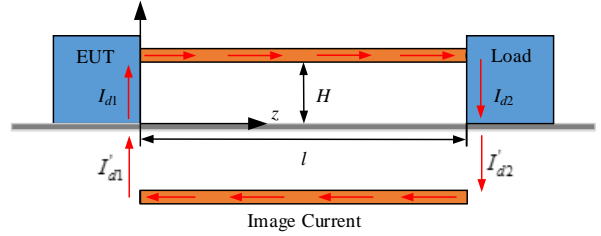


Fig. 6. A multi-dipole radiated model for cable-enclosure system.

According to the dipole antennas theory, the radiated field of all Hertzian dipole in Fig. 6 can be superimposed to obtain the radiated field E of a simple cable-enclosure system:

$$E = E_{TL} + E'_{TL} + E_{d1} + E'_{d1} + E_{d2} + E'_{d2}. \quad (18)$$

Where E_{TL} and E'_{TL} are the radiated fields from the real and mirror current of an interconnection cable, respectively, and E_{d1} and E'_{d1} are the radiated fields from the real enclosure panel and the mirror image of an EUT, respectively, and E_{d2} and E'_{d2} are the radiated fields from the enclosure panel and the mirror image of a load structure.

IV. RESULTS

A. Validation of the proposed method

In order to verify the proposed method, the model shown in Fig. 2 will be calculated via the method and the results will be compared with those from the full-wave software CST. The height of the cable from ground is $H = 50$ mm, the radius of the cable is $r = 1$ mm, the length of the internal cable of EUT and load case are $l_0 = l_4 = 0.02$ m, and the length of the interconnection cable is $l_2 = 2$ m.

The geometry and dimensions of the PCB consisting of a metallic trace, a substrate dielectric layer and a return path are shown in Fig. 7, where the trace is located at the middle of a PCB with dimensions of $w \times l \times t$ and conductivity $\sigma = 5.8 \times 10^7$ S/m. The dielectric substrate with dimensions of $a \times b \times h$ has a relative permittivity of $\epsilon_r = 4.3$. The size of the internal PCB of EUT is $a = 100$ mm, $b = 40$ mm, $l = 50$ mm, $w = 1$ mm, the PCB size of

the load enclosure is $a = 50$ mm, $b = 13$ mm, $l = 50$ mm, $w = 0.5$ mm, $t = 0.1$ mm, $h = 0.3$ mm.

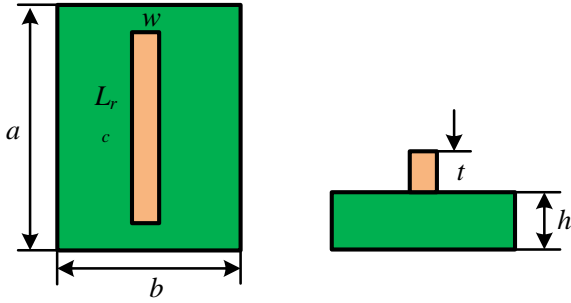


Fig. 7. The geometry and dimensions of PCB.

Figure 8 illustrates the current at the termination load calculated by the proposed method and CST simulation. The good agreement establishes the validation of the discontinuous penetrating cable model proposed in this paper. It should be noted that the result at low-frequency band of 0-500 MHz is better than that at higher frequency. The reason is that the highest frequency calculated accurately by the transmission line model is related to the height of the cable from the ground plane, which satisfies $h < \lambda/10$ [15], and higher order modes start to propagate along the cable.

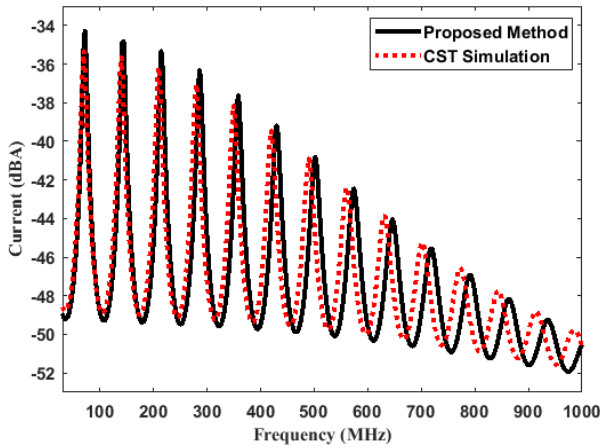


Fig. 8. Comparison of the current at the load end between the proposed method and CST simulation.

Figure 9 shows the comparison of the theoretically and numerically calculated radiated field ranging from 30 MHz to 1000 MHz at observation point P . It can be seen that the difference at most frequencies is less than 5 dB, and the calculation time for the radiated field is only 7s using the proposed method, which has an obvious speed advantage over CST simulation.

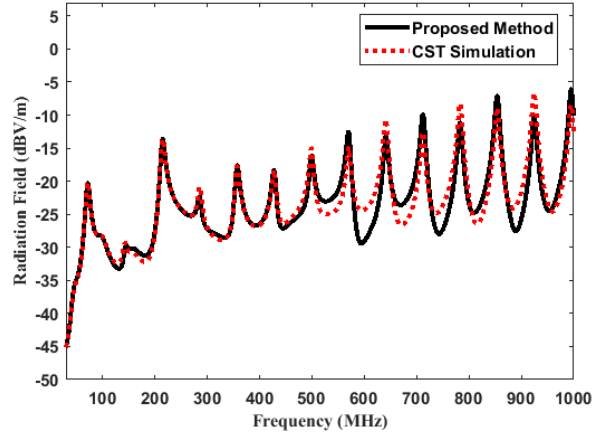


Fig. 9. Validation of radiation emission by comparing proposed method and CST simulation.

In Fig. 10, the solid line represents the current distribution at the load end in the presence of connectors, while the dotted line denotes the result of the transmission line without connectors. From the comparison, we can learn that the load end current will decay with the increase of frequency when connectors are taken into account. This can be attributed to the effect of connector's impedance and the bonding between the cable and connector, because the resistance and conductance varied with frequency reflect the loss of electromagnetic energy. Thus, the current at load end will decrease with the increase of frequency when connectors are included in the calculation.

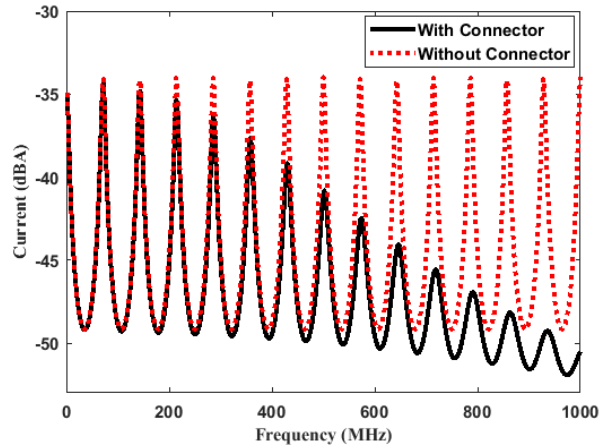


Fig. 10. A comparison of current distribution of load end with and without connectors.

B. Discussion

Because the connector can transmit signals, the transmission line theory can be used to study its distribution and transmission characteristics. As can be

seen in Fig. 11, the model of connector cascades a lot of identical *RLGC* units.

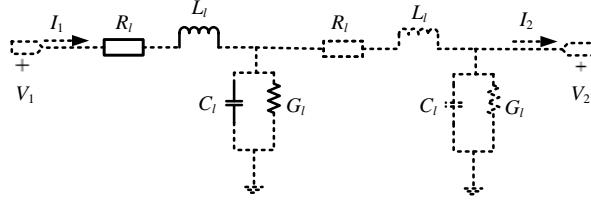


Fig. 11. The transmission line model of the connector.

In general, the characteristics of the transmission line can be represented by transmission (*ABCD*) matrix:

$$\begin{pmatrix} V_1 \\ I_1 \end{pmatrix} = \begin{pmatrix} A_l & B_l \\ C_l & D_l \end{pmatrix} \begin{pmatrix} V_2 \\ I_2 \end{pmatrix}. \quad (19)$$

The equivalent transmission line of connector has a propagation constant of γ_l and a characteristic impedance of Z_{cl} . The transmission parameter matrix is expressed as:

$$\begin{pmatrix} A_l & B_l \\ C_l & D_l \end{pmatrix} = \begin{pmatrix} \cosh(\gamma_l l_l) & Z_{cl} \sinh(\gamma_l l_l) \\ \sinh(\gamma_l l_l)/Z_{cl} & \cosh(\gamma_l l_l) \end{pmatrix}, \quad (20)$$

where l_l is the length of connector. Comparing (19) and (20), γ_l and Z_{cl} can be written as:

$$\gamma_l = \text{arcosh}(A_l)/l_l, \quad (21)$$

$$Z_{cl} = \sqrt{B_l/C_l}. \quad (22)$$

The scattering matrix is transformed into a transmission matrix by the transformation in (6). According to the definitions of γ_l and Z_{cl} , we obtain:

$$\begin{cases} R_l + j\omega L_l = \gamma_l Z_{cl} \\ G_l + j\omega C_l = \gamma_l / Z_{cl} \end{cases}. \quad (23)$$

RLGC parameters per unit length are derived as:

$$R_l = \text{Real}(\gamma_l Z_{cl}), \quad (24)$$

$$G_l = \text{Real}(\gamma_l / Z_{cl}), \quad (25)$$

$$C_l = \frac{\text{Im ag}(\gamma_l / Z_{cl})}{\omega}, \quad (26)$$

$$L_l = \frac{\text{Im ag}(\gamma_l Z_{cl})}{\omega}. \quad (27)$$

The parameters above are calculated by utilizing Matlab software and shown in Fig. 12. As shown in Fig. 12, the resistance, conductance, capacitance and inductance per unit length of connector are all strongly frequency dependent. The resistance and conductance increase with the increase of frequency, whereas the inductance and capacitance decrease with the increase of frequency. Since R_l and G_l reflect the loss of current in transmission process, the current in Fig. 10 will decrease

as the frequency increases when connectors are included in the model.

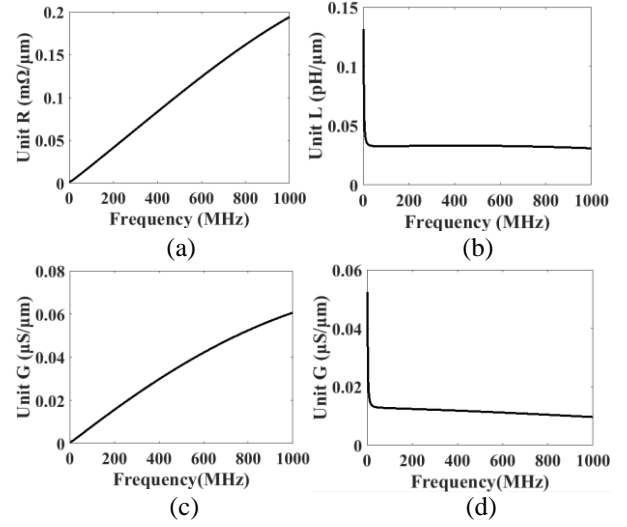


Fig. 12. *RLGC* parameters per unit length: (a) resistance per unit length; (b) inductance per unit length; (c) conductance per unit length; (d) capacitance per unit length.

VI. CONCLUSION

The interconnection cable between devices is usually an effective radiation antenna. In this paper, the influence of connectors on the signal transmission is considered in the calculation model. The proposed approach is verified by CST numerical analysis. The R_l and G_l of connector represent the loss during transmission, which determines the attenuation of the signal as it passes through the transmission path. The variation of connector's distribution parameters depend on the geometric design and the characteristics of the transmission material itself, which determines the voltage and current change produced by the signal when it flows through the transmission path. The results show that it is necessary to consider the influence of connector on signal current in the study of cable radiation.

ACKNOWLEDGMENT

This project is supported by the National Natural Science Foundation of China (Grant No 51675086).

REFERENCES

- [1] M. Meyer and P. Asfaux, "Radiated emissions modeling of a power cable [C]," *IEEE International Symposium on Electromagnetic Compatibility-EMC, Europe*, pp. 1-5, 2008.
- [2] J. Xu and Y. Lv, "Analysis of radiated emissions from multi-conductor lines [C]," *IEEE International Symposium on Antennas, Propagation and EM Theory*, pp. 1009-1012, 2008.
- [3] J. Jia, D. Rinas, and S. Frei, "Prediction of radiated

- fields from cable bundles based on current distribution measurements [C],” *IEEE International Symposium on Electromagnetic Compatibility (EMC EUROPE)*, pp. 1-7, 2012.
- [4] J. Jia, D. Rinas, and S. Frei, “An alternative method for measurement of radiated emissions according to CISPR 25 [C],” *IEEE International Symposium on Electromagnetic Compatibility (EMC EUROPE)*, pp. 304-309, 2013.
- [5] J. Wang, O. Fujiwara, and K. Sasabe, “A simple method for predicting common-mode radiation from a cable attached to a conducting enclosure [C],” *IEEE Asia-Pacific Microwave Conference APMC*, Taipei, pp. 1119-1122, 2001.
- [6] H. H. Park, H. B. Park, and H. S. Lee, “A simple method of estimating the radiated emission from a cable attached to a mobile device [J],” *IEEE Transactions on Electromagnetic Compatibility*, 55(2), pp. 257-264, 2013.
- [7] F. Costa, C. Gautier, B. Revol, et al., “Modeling of the near-field electromagnetic radiation of power cables in automobiles or aeronautics [J],” *IEEE Transactions on Power Electronics*, 28(10), pp. 4580-4593, 2013.
- [8] J. Meng, Y. X. Teo, D. W. P. Thomas, et al., “Fast prediction of transmission line radiated emissions using the Hertzian dipole method and line-end discontinuity models [J],” *IEEE Transactions on Electromagnetic Compatibility*, 56(6), pp. 1295-1303, 2014.
- [9] J. Meng, L. Zhang, J. Tang, et al., “Computation of radiated electric fields from cables using the 1D time-domain and frequency-domain TLM methods [C],” *IEEE International Conference on Electrical Machines and Systems*, pp. 3253-3258, 2015.
- [10] J. Jia, D. Rinas, and S. Frei, “Predicting the radiated emissions of automotive systems according to CISPR 25 using current scan methods [J],” *IEEE Transactions on Electromagnetic Compatibility*, 58(2), pp. 409-418, 2016.
- [11] H. W. Shim and T. H. Hubing, “Model for estimating radiated emissions from a printed circuit board with attached cables due to voltage-driven sources [J],” *IEEE Transactions on Electromagnetic Compatibility*, 47(4), pp. 899-907, 2005.
- [12] J. H. Goh, B. K. Chung, E. H. Lim, et al., “An improved model for estimating radiated emissions from a PCB with attached cable [J],” *Progress In Electromagnetics Research M*, 33, pp. 17-29, 2013.
- [13] C. R. Paul, *Analysis of Multiconductor Transmission Lines* [M], New York: John Wiley & Sons, pp. 45-54, 1994.
- [14] P. Xiao, P. A. Du, D. Ren, et al., “A hybrid method for calculating the coupling to PCB inside a nested shielding enclosure based on electromagnetic topology [J],” *IEEE Transactions on Electromagnetic Compatibility*, 58(6), pp. 1701-1709, 2016.
- [15] G. Ergaver and J. Trontelj, “Prediction of radiated emissions of automotive electronics early in the design phase based on automotive component level testing [J],” *Informacije MIDEM*, 46(1), pp. 42-52, 2016.
- [16] C. R. Paul, “Introduction to electromagnetic compatibility [J],” *IEE Review*, 38(7-8), pp.1-12, 1992.



Bing-Xue Zhang was born in Dezhou, Shandong province, China, in 1991. She received the B.E. from Harbin University of Science and Technology in 2014.

She is currently a Master student of UESTC. Her research interest is numerical methods of electromagnetic radiation from interconnecting cables.



Pei Xiao was born in Shaoyang, Hunan province, China, in 1989. He received the Bachelor of Mechanical Engineering degree from UESTC, Chengdu, China, in 2013. He is currently a Ph.D. student at UESTC.

His research interests are numerical computation, theoretical electromagnetic analysis including the EMT method, and EMC/EMI in Multi-conductor transmission line (MTL).



Dan Ren was born in Huainan, Anhui Province, China, in 1986. He received the Bachelor of Industrial Engineering degree and the Ph.D. degree in Mechatronics Engineering from the University of Electronic Science and Technology of China, Chengdu, China, in 2011 and 2017, respectively.

He is also a Visiting Student in the UBC Radio Science Lab, Vancouver, BC, Canada. His research interests include numerical computation, electromagnetic measurement, electromagnetic simulation, and EMC/EMI in shielding enclosures, apertures, and cable radiation.



Ping-An Du received the M.S. and Ph.D degrees in Mechanical Engineering from Chongqing University, Chongqing, China, in 1989 and 1992, respectively.

He is currently a Full Professor of Mechanical Engineering at the University of Electronic Science and Technology of China, Chengdu, China. His research interests include numerical simulation in EMI, vibration, temperature, and so on.